High Power CO_2 Laser Welding of Thick Plate†
— Multipass Weding with Filler Wire —

Yoshiaki ARATA*, Hiroshi MARUO**, Isamu MIYAMOTO*** and Ryoji NISHIO****

Abstract

Multipass laser welding technique using filler wire was developed. Welding parameters were optimized, which include assist gas pressure, wire feeding position, wire feed rate and gap width. Wire-laser beam interaction, plasma ignition and growth, metal transfer and energy coupling ratio of the wire in free spece and the work in the gap during bead formation were analyzed. Based upon these results, multipass welding of thick plate was demonstrated.

KEY WORDS: (Multipass Welding) (Filler Wire) (Laser Plasma) (Assist Gas) (Single Pass Welding) (Butt Welding) (Beam Coupling Ratio) (Welding Phenomena) (Laser Welding)

1. Introduction

CO_2 lasers provide excellent welding characteristics in comparison with conventional arc welding due to their high power density, and are much more useful than the electron beam from the practical view points of their easiness in automatic controlling and ability to send beam energy to distant place at atmospheric pressure. The disadvantage of laser welding is, however, to produce plasma which absorbs and/or scatters the incoming laser beam[1,2] especially at low welding speeds, resulting in much shallower penetration depth than electron beam welding. Thus industrial applications of laser welding are limited to rather thin plate in range of 0.2 – 6 mm in thickness[3], and the thicker plates than 20 mm have not been welded so far by industrial CO_2 lasers.

There is a lot of work for increasing penetration depth in laser welding. Assist gas technique, in which inert gas is directed to the laser-material interaction position, was shown to increase penetration depth[1], and control mechanism of the plasma above the work surface and optimum gas assisting conditions were also reported[4]. However, the weldable thickness of given laser powers with plasma control is very small in comparison with electron beam welding of the same powers, 15 – 20 mm at 10 kW power level of laser beam, for instant as shown in **Fig. 1**[5]. Recently it was found that 40 mm thick plate can be laser welded in vacuum of 10^{-3} – 10^{-4} Torr at 10 kW power level[6]. And influence of laser plasma remaining in the beam hole on penetration depth was analyzed[8] that the penetration depth is limited by laser produced plasma existed in cavity (beam hole) as for

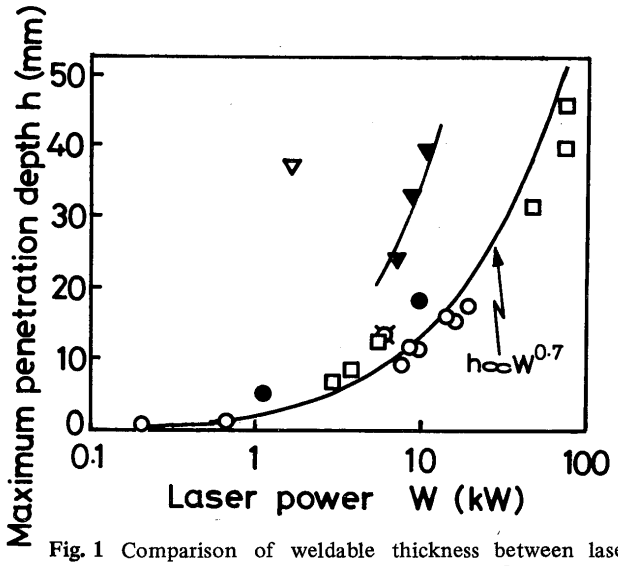

Fig. 1 Comparison of weldable thickness between laser welding and electron beam welding. ○ (Low alloy steel) □ (Stainless steel)-◇-(Non vac EB)[5] ● (Stainless steel)[4] ▼ (Vac LB)[6], ▽ (Vac EB)

welding at atmospheric pressure and penetration depth increased due to thin plasma in beam hole at lower pressure.

In order to overcome this limitation subjected to laser welding in the atmospheric pressure, the authors have developed multipass laser welding with filler wire feeding for welding thick plate.

Filler wire technique has been used for welding thin plate in steel production line[8]; the wire is fed to the beam-work interaction position at the work surface for enlarging the fit-up-tolerance and improving the metallurgical properties of the joint by the addition of metal

† Received on Nov. 5, 1986
* Professor
** Professor, Faculty of Engineering, Osaka Univ.
*** Assistant Professor, Faculty of Engineering, Osaka Univ.
**** Graduate Student

Transactions of JWRI is published by Welding Research Institute of Osaka University, Ibaraki, Osaka 567, Japan

elements. On the other hand in this procedure, wire is fed directly into the gap and so molten filler material fills the gap with minimal melting of the base material. Thus when this technique is combined with multipass welding technique, there is no limitation in weldable thickness, in principle. In the present paper, multipass laser welding of thick plate is described; interaction between CO_2 laser and wire, and bead formation in the gap are discussed.

2. Experimental Apparatus

High power CO_2 laser beam from unstable resonator with magnification ratio of 1.5 (AVCO HPL-10) was focused by f/7 telescope or f/7 concave spherical mirror system as shown in **Fig. 2**. Focal points and beam diameters of focused laser beam by these two optical systems were determined by acrylic method[9]. The focused laser beam diameter of spherical mirror system is 0.56 mm providing high energy density of $4.7 \times 10^6 W/cm^2$, though that of telescope is 1.0 mm and $1.3 \times 10^6 W/cm^2$ by the significant astigmatism. The laser power was fixed at 10 kW in all experiments.

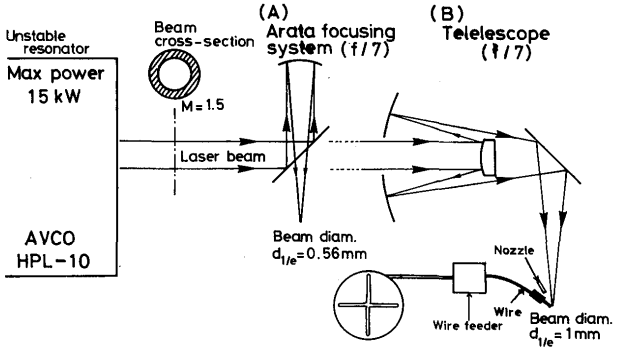

Fig. 2 Schematic illustration of laser generator and focusing systems.

Assist gas, He or Ar, was directed to wire-laser interaction point to control the laser-produced plasma by using a copper nozzle of 1 mm in internal diameter which was set 60 degrees respect to the horizontal line, and the total pressure of assist gas was measured at the point on wire surface acrossing the focal point. In the free space of Ar gas atmospher, beam wire interaction was studied in some detail by using a 35 mm camera, a high speed color video (200 fps) and a high speed camera (3000 fps). Direction and power of reflected beam from wire edge were measured by PMMA plates surrounding wire beam interaction point and a corn power meter respectively.

As shown in **Fig. 3**, filler wire of 1.6 – 2.0 mm in diameter was fed into the gap of butt welding joint with an angle of 45 degrees respect to the work surface by using commercially available wire feeder. Welding was carried out in Ar atmosphere by using a shielding box with a narrow slit for beam inlet at the top and a glass window on the side for observation.

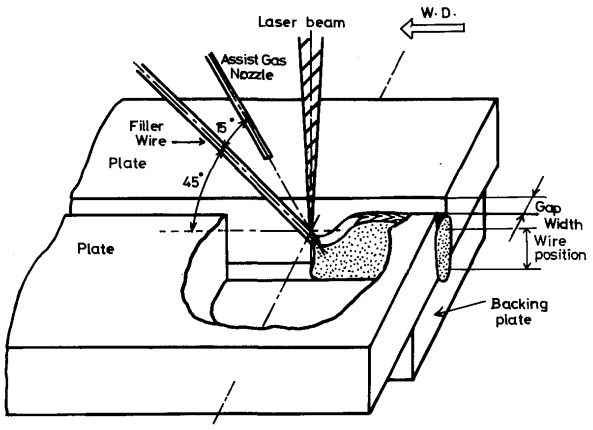

Fig. 3 Schematic illustration of single pass welding with filler wire.

0.2% carbon steel (SM41A) and the wire of 1.0 – 2.0 mm in diameter (YGW11), were used in this experiment.

3. Results and Discussion

3.1 Wire-beam interaction

First of all, the wire was melted by focused CO_2 laser beam in free space of air or inert gas atmosphere. Very bright plasma was observed providing very small value of melt wire volume. Two different types of plasma, pink and blue, were seen as shown in **Fig. 4**; larger pink plasma ball is plasma of Ar gases, and was seen to semi-periodically detach from the wire surface to move up, disappearing at a height of several centimeters along the beam axis. This plasma interacts with incoming laser beam and absorbs the beam energy. Blue plasma, which ejects perpendicularly to the incoming wire surface, is metal vapor plasma, and was not seen to interact with the laser beam. So it was found that the atmospheric gas plasma had to be suppressed to get sufficient melting of wire. When the assist gas, Ar or He, was directed to the beam-wire interaction point, the brightness of the atmospheric gas plasma was diminished, and disappeared at all with increasing assist gas pressure eventually. The proper pressure of assist gas was just a value of suppressing atmospheric gas plasma to disappear as shown in **Fig. 5**.

The wire melting phenomena were rather different between the cases of using spherical mirror and of using telescope due to their focused beam diameters. Wire stick-out phenomena, beam passing through the wire to form a small beam hole in the wire and wire sticking out 2 – 4 mm furthermore from wire-beam interaction point to melt finally, was observed as shown in **Fig. 6** (a) when spherical mirror system was used. Such wire stick-out phenomenon was not observed in case of using tele-

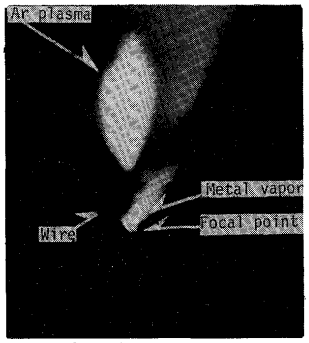

Fig. 4 Laser plasma, atmospheric plasma and metal vapor plasma.

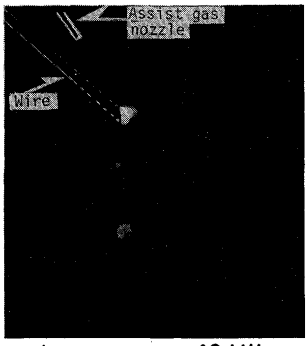

Fig. 5 Plasma suppression by assist gas.

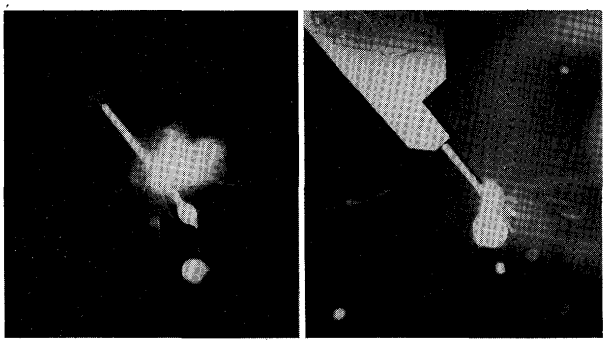

Fig. 6 Wire melting phenomena.

scope (b), though formation of a small beam hole in molten droplet was seen intermittently. This wire stick-out phenomenon was observed at high laser energy density of 4.7×10^6 W/cm^2 and also tended to be seen when wire of larger diameter was used. This cause is that the drilling speed of laser beam is much higher than the entire wire melting speed by thermal conduction. This is thought to be the disadvantage for this welding procedure because wire setting would be out of order if wire bumps against the bottom of weld gap. The maximum wire diameter, thus, was limited to 2 mm. Molten droplets of 2 – 6 mm in diameter, three or four times lager than wire diameter, were formed to fall down periodically.

As shown in Fig. 7, the critical wire fed volume v_{FC}, above which no wire droplet is produced continuously in free space, is plotted against assist gas pressure and shows the influences of the focused beam diameter and the kinds of assist gas, He or Ar. No significant difference in v_{FC} was seen between Ar and He for both shielding and assist gases; He and Ar gases were used for plasma controlling and shielding respectively, hereafter. The v_{FC} increases with increasing assist gas pressure, and the maximum value of v_{FC} about 240 mm^3/sec is attained at 40 – 60 mmAq by

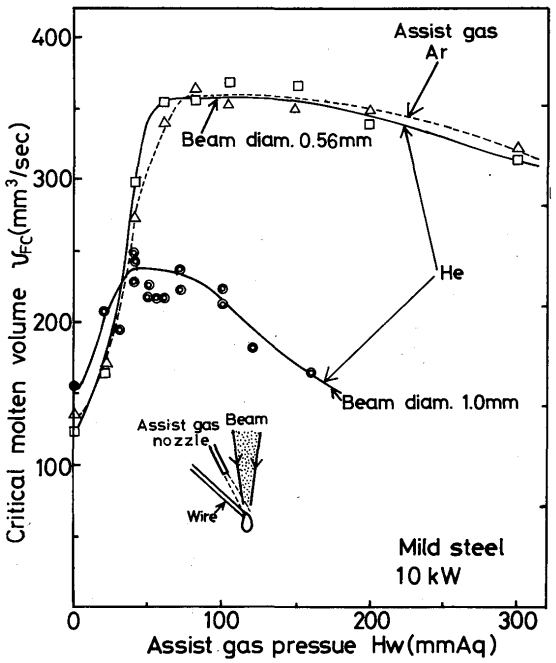

Fig. 7 Critical wire fed volume vs. assist gas pressure.

using f/7 telescope. At pressures higher than 70 mmAq, v_{FC} tends to decrease probably due to the cooling effect of the assist gas. The maximum value of v_{FC} for f/7 spherical mirror was found to be 1.5 times larger than that of telescope and was approximately 360 mm^3/sec.

The surface temperature of molten droplet was measured through a narrow slit, which only the radiation from molten droplet passed through, by the radiation pyrometer corrected by the W-Re thrmo-couple as shown in Fig. 8. The radiation coefficient E of the measured wire was 3.5. It was found that molten droplet was overheated up to 2800°C, which was just below the temperature of vaporization, when wire fed volume was small. As increasing wire fed volume, the temperature of droplet became

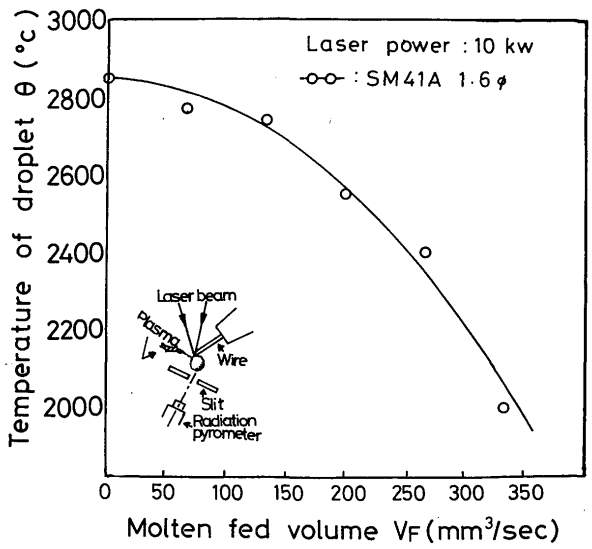

Fig. 8 Surface temperature of molten droplet vs. wire fed volume.

lower, though it was 2000°C being much overheated from its melting point even at the critical wire fed volume. Then assuming that the temperature of molten droplet is uniform, the beam coupling ratio of the molten droplet A is estimated by **Equation (1)** and is shown in **Fig. 9**:

$$A = v_{FC}\rho(C\theta+H_m)/W_b+4\pi r^2 E\sigma(\theta+273)^4/W_b \quad (1)$$

where W_b is input beam power, v_{FC} critical wire fed volume, c specific heat, ρ density, θ temperature of molten wire, Hm latent heat, r radius of droplet, E mean radiation coefficient and σ Stephan-Boltsman coefficient. When higher energy density beam by using spherical mirror system was used, the coupling ratio approximately 50% was obtained as the maximum value. Main loss of the laser beam is due to the reflection from wire edge and the passing through the wire. The coupling ratio thus estimated are much higher than the normal absorptivity of CO_2 laser beam to steel, 10 – 15% of incident laser power. Higher coupling ratio is thought to be due to multiple reflections of laser beam in the cavity formed in molten droplet or in wire.

Energy and direction of reflected beam from wire edge were analyzed by acrylic burn pattern and corn power meter using 2.0 mm diameter wire. Assist gas pressure was set to a pressure of 40 mmAq, the optimum value to suppress the laser plasma. The wire-beam interaction point was surrounded with acrylic plates except the narrow slit for laser beam and wire torch inlet with enough distance from plates to the wire-beam interaction point for eliminating the influence of the heat by metal vapor plasma. Conical laser beam reflects from the wire edge in a direction range from horizontal to somewhat downward was observed as illustrated in **Fig. 10**. As the wire feed rate increases, the reflected laser power increases and the power passed through the wire decreases. The reflected power saturates to be a constant value of 35% of incident laser power in the range of the wire feed rate faster than

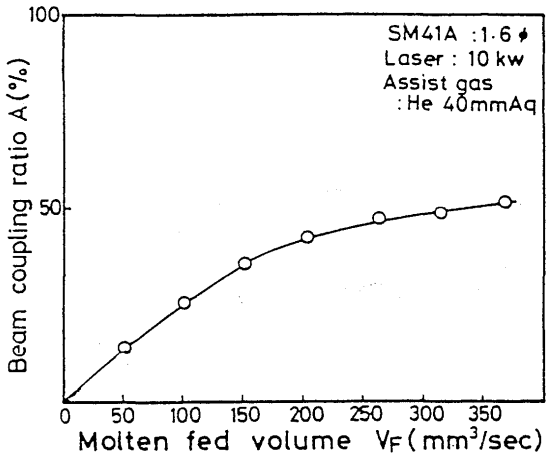

Fig. 9 Beam coupling ratio vs. wire fed volume.

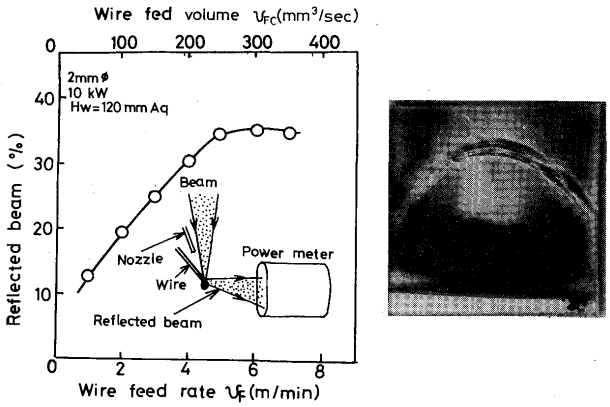

Fig. 10 Power and burn pattern of reflected beam from wire edge.

5 m/min. Thus at the critical wire feed rate, 50% of incident laser power is absorbed by wire and 35% in reflected to loss. 15% of incident laser power is thought to be lost by passing through beam and the heat carried away by metal vapor plasma etc. Burn pattern of reflected beam consists of the somewhat crescent shaped pattern and the bowl shaped pattern. The crescent shaped pattern is formed by the reflected beam from the unmelted wire edge. And the bowl shaped pattern is formed by the reflected beam from the molten droplet. The photograph in Fig. 10 is the burn pattern at the critical wire feed rate and the beam power from the molten droplet is stronger than that from the unmelted wire edge. The ratio of these two reflected beam is 3 to 7. This also suggests that much laser power heats up the molten droplet increasing temperature from its melting point even at the critical wire feed rate.

The critical melt wire volume for various wire diameter (1.0 – 2.0 mm) is plotted against the misalignment of the laser beam ΔY with respect to the wire center in **Fig. 11**. The maximum melt volume of 1.6 and 2.0 mm diameter wire is about 350 – 360 mm^3/sec. Tolerance of the misalignment of the laser beam in case of 2.0 mm diameter wire is half of 1/e beam radius (0.25mm) in which range the maximum melt volume is obtained constantly, though v_{FC} decreased down to 70% of the center when the misalignment is larger than 0.25 mm in case of using 1.6 mm diameter wire. When wire diameter is as small as 1.2 or 1.0 mm, melting volume decreased by wire fluctuation. Then wire of 1.6 or 2.0 mm diameter was used. Influence of focusing position ΔZ with respect to the wire surface is shown in **Fig. 12**. The maximum value of v_{FC} is obtained when wire surface is located at the focal point. Though wire was located 2 – 4 mm above or below from focal position where beam diameter was larger than that of focal point, tolerance of the misalignment of the laser beam ΔY for a constant wire feed rate did not

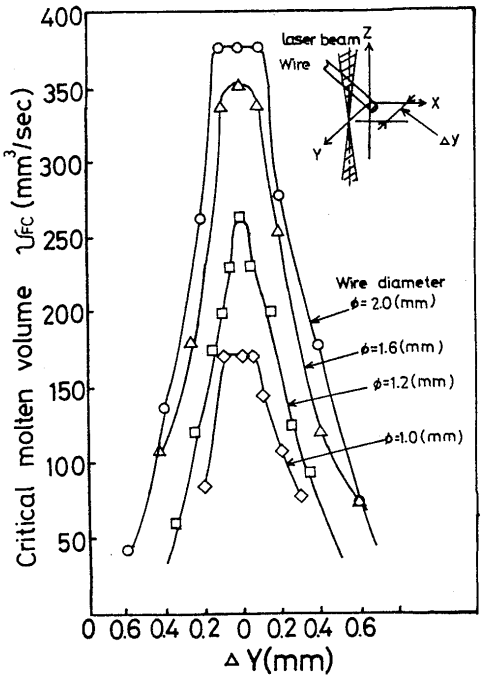

Fig. 11 Critical melt wire volume vs. misalignment of laser beam at various wire diameter.

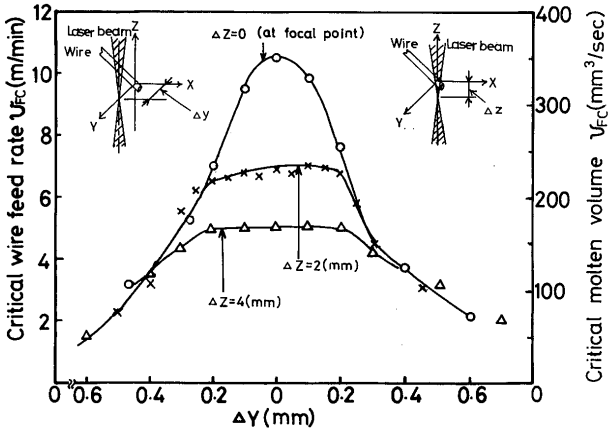

Fig. 12 Critical melt wire volume vs. misalignment of laser beam at various focasing position.

change.

3.2 Bead formation in single pass welding

Welding was performed with filler wire feeding into the parallel gap at the middle of the plate thickness. Typical bead cross sections at various assist gas pressure are shown in **Fig. 13**. When the assist gas pressure was below 30 mmAq, insufficient plasma suppression caused bright plasma existence in the gap, and wine-cup bead of the wide melt width at the surface with reduced penetration depth and luck of fusion near the gap bottom was produced. At assist gas pressure of 40 – 60 mmAq, which is as high as the aforementioned range of the optimum pressure in wire heating in the free space, the molten filler metal filled up the throughout the plate thickness without any lack of fusion. At pressures higher than 70 mmAq,

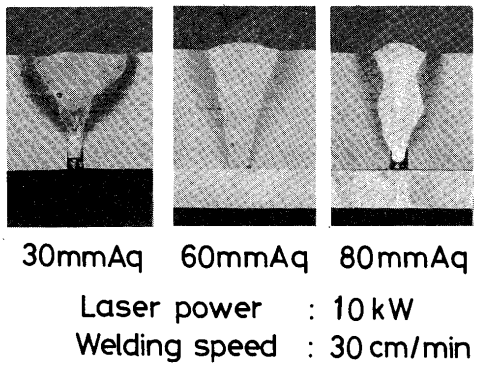

Fig. 13 Typical bead shapes at various assist gas pressure.

bead width became wider around the beam-wire interaction position with accompanying lack of fusion near the bottom again.

Brief estimation of absorbed laser power in the work was analyzed from bead dimensions by assuming a line heat source moving in an infinite body[10]. Then the coupling ratio A was calculated as follow;

$$A = 8kT_m(0.2 + dV_b/4K_d)h_p/W_b \quad (2)$$

where k is the thermal conductivity of material, K_d the thermal diffusivity of the material, T_m melting point of the material, d mean bead width, V_b welding speed, h_p deposition height and W_b incident laser power. Results are plotted against assist gas pressure in **Fig. 14** with beam coupling ratio in free space for comparison. The maximum beam coupling ratio in the work is about 80% and there is no difference between the two focusing systems, though it varied from 30% to 50% in free space according to the focused beam diameter. And also no significant difference was seen in the resultant beads. This fact sug-

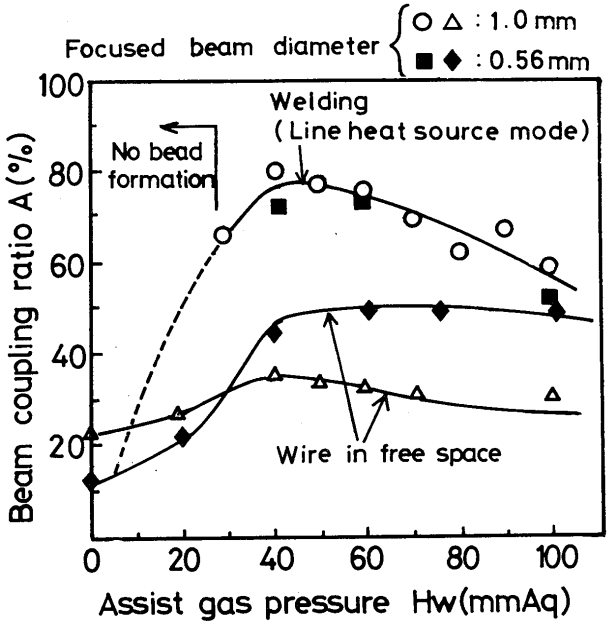

Fig. 14 Thermal efficiency for bead formation vs. assist gas pressure.

gests that the lost energy in free space by the reflected beam or the passed beam through wire is absorbed by the base metal or deposited metal by a certain mechanism. And furthermore it means that this procedure does not require excellent focusibility to lasers unlike the case of autogenous welding. High efficiency welding can be performed even lasers with poor focusibility such as multimode lasers or lasers with small magnification factors.

Bead cross sections at three different vertical positions of wire-beam interaction point when deposition height was relatively high; 14 mm, are shown in **Fig. 15**. Too low wire position caused that the molten metal flow facing to the wire edge hanged over the wire-beam interaction point intermittently to block the incident laser beam resurting unmelted wire remaining in the deposited metal as shown in (c). Luck of fusion, however, was produced at higher wire position relative to deposition height as show in (a). Such weld defects were not formed when wire position was located around the middle part of deposition height in any welding condition tested in this procedure.

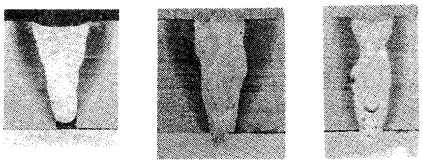

Fig. 13 Bead cross section at three different vertical positions of wire-beam interaction position.

Welding was performed at gap width of 2.5 mm at various combinations of welding speeds and wire feed rates to obtain the same deposition height as shown in **Fig. 16**. Sound bead is obtained at slower welding speed than 50 cm/min. At faster welding speeds, lack of fusion at the bottom occurred. In order to understand beam material interaction and molten metal transfer to base metal in the gap, welding phenomena were observed from the side with removing one of the plates as shown in **Fig. 17**. The typical photograph at the optimum welding speed is shown in (a). Molten wire is seen to contact the side plate and transfer continuously, and the beam passing through the wire is absorbed and reheats molten metal and the bottom to melt around the bottom sufficiently. Behind the wire beam interaction point, cavity is formed by the wire edge, side plate and molten metal flow, and the reflected beam from wire edge is absorbed again, which causes the high welding efficiency up to 80%. The photograph at rather high welding speed is shown in (b). Wire stick-out and less heating of the bottom by the passed

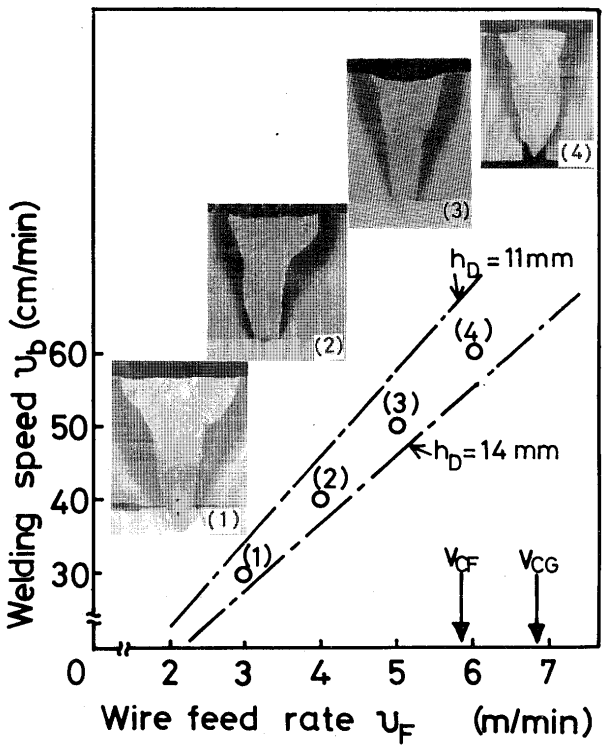

Fig. 16 Bead cross sections at various conbination of welding speed and wire feed rate.

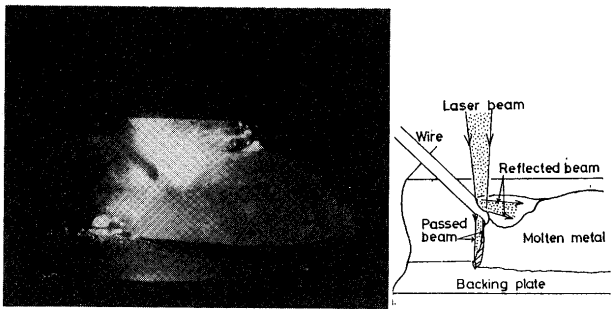

(a) Welding speed : 30 cm/min
Laser power : 10 kW
Filler wire : Mild steel (2.0mm ϕ) 5 m/min

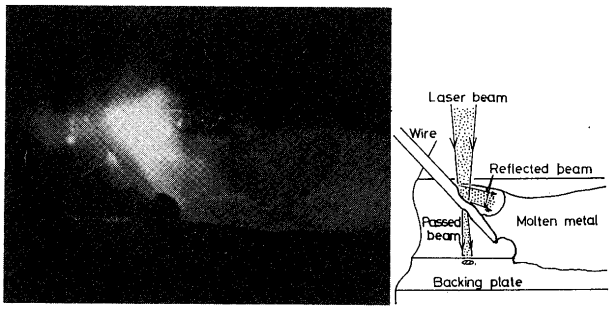

(b) Welding speed : 50 cm/min
Laser power : 10 kW
Filler wire : Mild steel (2.0mm ϕ) 5 m/min

Fig. 17 Welding phenomena at different welding speeds.

through beam, because the passed beam heats only the center of backing plate without sufficient time for thermal conduction to the corner, are seen in comparison with

(a). This means that the formation of lack of fusion is caused by the poverty of additional heating by the passed through beam. Sound bead without luck of fusion at the bottom can be obtained by controlling welding speed, wire fed volume and wire position, which influence the passed through beam and the heat input to the bottom. And also welding at much higher welding speeds is thought to be possible by increasing heat input to the bottom by the additional heat source such as joule heating of wire or argumentation of arc.

3.3 Multipass welding of thick plate

2 passes welding of 25 mm thick plate was performed at first. First layer was weld by autogenous welding; assist gas pressure was set to 120 mmAq which was the optimum value in case of the autogenous welding at welding speed of 40 cm/min. Second layer with 3 mm gap width was weld at rather slow wire feed rate to obtain sufficient overlap to the first layer. Sound bead without any weld defect was obtained as shown in **Fig. 18**. Welding with 2 passes is possible up to 30 mm thick plate in this procedure.

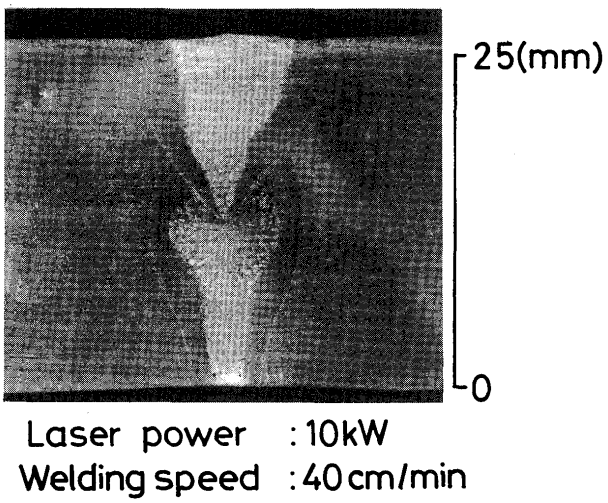

Fig. 18 Cross section of 25 mm thick plate joined by 2 pass butt welding. v_b = 40 cm/min.

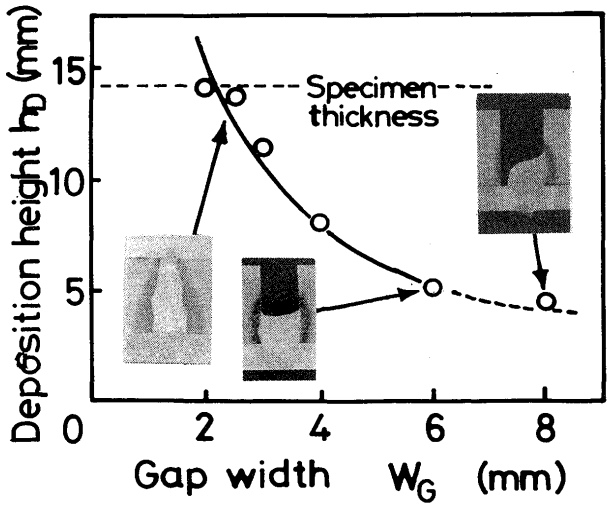

Fig. 19 Deposited bead hight vs. gap width at fixed wire feed rate, 6 m/min.

The deposition height against gap width at the fixed wire feed rate (6 m/min) of 1.6 mm diameter wire is shown in **Fig. 19**. Deposition height is seen to be approximately in inverse proportion to the gap width due to small shrinkage deformation. Bead deposition without weld defects was obtained in a range of gap width of 2 – 6 mm within the conditions tested. A gap width of 2 mm is the narrowest for the smooth feeding of 1.6 mm diameter wire into the gap. And a gap width of 6 mm is the maximum width for sound deposition, above which lack of fusion tends to be formed between side plate and deposited metal. Then the maximum weldable thickness is determined by a simple calculation.

$$t_{max} = t_{aut} + W_{gc} \cdot f \tag{3}$$

where t_{aut} is the thickness of the first layer by autogenous welding, W_{gc} the critical gap width without any defect and f is the f-number of the focusing system. Using t_{aut} = 15 mm, W_{gc} = 6 mm and f = 7, the maximum weldable thickness was calculated to be 57 mm, then welding of 50 mm thick plate was performed. The joint geometry prepared and the cross section of resultant bead are shown in **Fig. 20**. Welding was performed by 5 passes at welding speed of 35 cm/min using 1.6 mm diameter wire, showing bead width of approximately 7 mm corresponding to an aspect ratio of about 7. A bead height of 30 mm is seen to be formed by the first two layers. The last 20 mm in thickness was weld with 3 passes for sufficient overlapping. It should be noticed that welding of up to 50 mm thick plate is possible by using the 10 kW class laser and this thickness requires approximately 100 kW laser power in autogenous welding.

4. Conclusions

Multipass laser welding technique with filler wire was developed using 10 kW class laser and demonstrated joining of thick plate up to 50 mm. Wire-beam interaction, beam coupling ratio to the wire and the work were analyzed. The plasma suppression technique and welding parameters were discussed for optimization. The followings are the conclusions obtained.

(1) Two kinds of plasma, atmospheric gas plasma and metal vapor plasma, were observed existing along the beam path and ejecting perpendicularly to the wire surface respectively. The assist gas technique is sufficient to suppress laser plasma and the critical melt volume of wire increased 2.5 – 3 times in comparison with the case of no plasma suppression.

(2) At the critical wire feed rate, 50% of incident laser power is absorbed by wire and 35% is lost by the

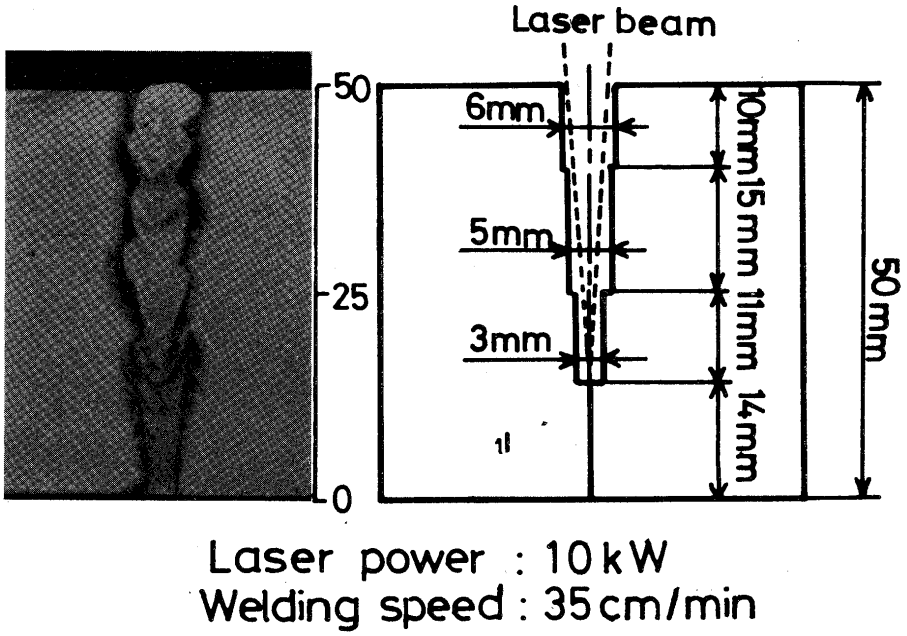

Fig. 20 Bead cross section for 50 mm thick plate for multipass welding. v_b = 35 cm/min.

reflection in the wire-beam interaction in free space. The rest 15% is lost by the beam passed through wire and the heat carried away by the metal vapor plasma. The maximum beam coupling ratio in welding, however, is about 80% and is higher than that in free space because beams passed through wire and the reflected from wire edge are absorbed again in the gap.

(3) This welding procedure does not require excellent focusibility to lasers unlike the case of autogenous welding, and high efficiency welding can be performed even lasers with poor focusibility such as multimode lasers or lasers with small magnification factors.

(4) Mild steel of 50 mm thick plate, which requires 100 kW class laser in single pass welding, was weld with 5 passes at 10 kW power level with satisfactory good bead geometry.

Acknowledgements

The authors are grateful to Mr. T. Oda and associate professor M. Tomie for his wholehearted cooperation and kindly advice for this research work.

References

1) Locke, E. V., E. D. Hong, and R. A. Hella, (1972) IEEE J. Quan. Elec., Vol. QE-8, 2, 132–135.

2) Arata, Y., N. Abe, and T. Oda, (1983). Prc. ICALEO'83, Vol. 38, 59–66.

3) Kawai, Y., M. Aihara, K. Ishii, M. Tabuchi, and H. Sasaki, (1984). Kawasaki steel tech. rept., No. 10, 39–46.

4) Miyamoto, I., H. Maruo, and Y. Arata, (1984). Prc. ICALEO-'84, Vol. 44, 68–75.

5) Banas, C. M., (1976). Final report under Naval Research Lab., Contract N00173-76-M-0107 UTRC Rept. No. r76-912260-1.

6) Arata, Y., N. Abe, and T. Oda, (1984). Prc. ICALEO'84. Vol. 44, 1–7.

7) Maruo, H., I. Miyamoto, T. Ooie and M. Yosida, (1986). Preprints of National Meeting of JWS, Vol. 39, No. 103 (in Japanese).

8) Sasaki, H., N. Nishiyama, and A. Okada, (1983). Prc. 3rd. CISFFEL, 569–576.

9) Miyamoto, I., H. Maruo, and Y. Arata, (1984). Prc. ICALEO-'84, Vol. 44, 313–320.

10) Wells, A. A., (1952). W. J., Vol. 31, s263–s267.